

## FLEXIBLE SUSPENSIONS WITH A HEXAGONAL EQUATOR

VICTOR ALEXANDROV AND ROBERT CONNELLY

ABSTRACT. We construct a flexible (non-embedded) suspension with a hexagonal equator in Euclidean 3-space. It is known that the volume bounded by such a suspension is well defined and constant during the flex. We study its properties related to the Strong Bellows Conjecture which reads as follows: if a, possibly singular, polyhedron  $\mathcal{P}$  in Euclidean 3-space is obtained from another, possibly singular, polyhedron  $\mathcal{Q}$  by a continuous flex, then  $\mathcal{P}$  and  $\mathcal{Q}$  have the same Dehn invariants. It is well known that if  $\mathcal{P}$  and  $\mathcal{Q}$  are embedded, with the same volume and the same Dehn invariant, then they are scissors congruent.

### 1. Introduction

A polyhedron (more precisely, a polyhedral surface) is said to be *flexible* if its spatial shape can be changed continuously due to changes of its dihedral angles only, i.e., in such a way that every face remains congruent during the flex.

Flexible polyhedra homeomorphic to a sphere in Euclidean 3-space were originally constructed by R. Connelly in 1976 [8]. Later, many properties of flexible polyhedra were discovered, for example:

(1) In 1985, R. Alexander [1] proved that *every flexible polyhedron in Euclidean  $n$ -space,  $n \geq 3$ , preserves the following quantity*

$$\sum \varphi(F) \operatorname{vol}_{n-2}(F)$$

---

Received June 7, 2009; received in final form July 11, 2010.

The first author receives support from the Russian Foundation for Basic Research (grant 10-01-91000-ANF) and the Federal Program ‘Research and educational resources of innovative Russia in 2009–2013’ (contract 02.740.11.0457). Research of the second author is supported in part by NSF Grant DMS-0209595.

2010 *Mathematics Subject Classification*. Primary 52C25. Secondary 51M20, 14H50.

called its *total mean curvature*. Here, summation is taken over all  $(n-2)$ -faces  $F$  of the polyhedron,  $\text{vol}_{n-2}(F)$  denotes the  $(n-2)$ -volume of  $F$ , and  $\varphi(F)$  denotes the dihedral angle between the two  $(n-1)$ -faces adjacent to  $F$ . Later it was shown by several authors that invariance of the total mean curvature is a consequence of the Schläfli differential formula, see, for example, [3].

(2) In 1996, I. Kh. Sabitov [15] proved that *every flexible polyhedron in Euclidean 3-space preserves its oriented volume during the flex* and, thus, gave a positive answer to the Bellows Conjecture. An improved presentation is given in [16]; another proof is published in [9].

On the other hand, many interesting problems related the flexible polyhedra still remain open. For example, in a comment added to the Russian translation of [7] R. Connelly conjectured that *if a, possibly singular, polyhedron  $\mathcal{P}$  in Euclidean 3-space is obtained from another, possibly singular, polyhedron  $\mathcal{Q}$  by a continuous flex, then  $\mathcal{P}$  and  $\mathcal{Q}$  have the same Dehn invariant. (We will define the Dehn invariant later.) If  $\mathcal{P}$  and  $\mathcal{Q}$  are embedded and have the same Dehn invariant and enclosed volume, then they are scissors congruent, i.e.,  $\mathcal{P}$  can be divided into a finite set of tetrahedra each of which can be moved independently one from another in 3-space in such a way that the resulting set constitutes a partition of  $\mathcal{Q}$ . We call this the *Strong Bellows Conjecture*.*

Studying scissors congruence one should obviously take into account some classical results on Hilbert's Third Problem that read as follows: *two embedded polyhedra in Euclidean 3-space are scissors congruent if and only if they have the same volume and every Dehn invariant takes the same value for those polyhedra*, see [6], [10]. Thus, if two embedded polyhedra  $\mathcal{P}$  and  $\mathcal{Q}$  are such that one is obtained from the other by a continuous flex, and the Strong Bellows Conjecture were true, then  $\mathcal{P}$  and  $\mathcal{Q}$  would be scissors congruent. But, alas, the Strong Bellows Conjecture is not true, although the question whether the Strong Bellows Conjecture is true for embedded polyhedra remains open.

Our main results are as follow.

In Section 3, we construct a new example of a flexible polyhedron (with self-intersections) in Euclidean 3-space, namely, a flexible suspension with a hexagonal equator. Actually, this is the first example of a (singular) flexible suspension with a hexagonal equator. Moreover, we do not know any non-trivial example of a flexible suspension with a pentagonal equator.<sup>1</sup>

In Section 4, we prove that the Strong Bellows Conjecture is wrong for the flexible suspension with a hexagonal equator constructed in Section 3. In fact,

---

<sup>1</sup> In this paper, we do not study flexible suspensions with pentagonal equators and don't describe when they are trivial. Nevertheless, let us give an example: fix an interior point on an edge of the equator of a flexible octahedron (treated as a suspension with a quadrangular equator), declare it the fifth vertex of the equator, and add two edges joining the fifth vertex of the equator with the north and south poles of the suspension. The resulting suspension is flexible, but trivial.

this is the first example of a flexible (embedded or not) polyhedron where the Strong Bellows Conjecture does not hold.<sup>2</sup>

### 2. A description of flexible suspensions

Our study of flexible suspensions is based on the fundamental flexibility equation derived in [7]. In this section, we briefly review the notation and facts which are important for us.

**Basic definitions.** A map from a simplicial complex  $K$  to Euclidean 3-space  $\mathbb{R}^3$ , linear on each simplex of  $K$ , is called a *polyhedron*. If the vertices of  $K$  are  $v_1, \dots, v_V$ , and if  $\mathcal{P} : K \rightarrow \mathbb{R}^3$  is a polyhedron, then  $\mathcal{P}$  is determined by the  $V$  points  $p_1, \dots, p_V$ , called the *vertices* of  $\mathcal{P}$ , where  $\mathcal{P}(v_j) = p_j$ .

If  $\mathcal{P} : K \rightarrow \mathbb{R}^3$  and  $\mathcal{Q} : K \rightarrow \mathbb{R}^3$  are two polyhedra, then we say  $\mathcal{P}$  and  $\mathcal{Q}$  are *congruent* if there is an isometry  $A : \mathbb{R}^3 \rightarrow \mathbb{R}^3$  such that  $\mathcal{Q} = A \circ \mathcal{P}$ , i.e., which takes each vertex of  $\mathcal{P}$  to the corresponding vertex of  $\mathcal{Q}$ ,  $q_j = A(p_j)$  or equivalently  $\mathcal{Q}(v_j) = A(\mathcal{P}(v_j))$  for all  $j = 1, \dots, V$ . We say  $\mathcal{P}$  and  $\mathcal{Q}$  are *isometric* if each edge of  $\mathcal{P}$  has the same length as the corresponding edge of  $\mathcal{Q}$ , i.e., if  $\langle v_j, v_k \rangle$  is a 1-simplex of  $K$  then  $|p_j - p_k| = |q_j - q_k|$ , where  $|\cdot|$  stands for the Euclidean norm in  $\mathbb{R}^3$ .

A polyhedron  $\mathcal{P}$  is *flexible* if, for some continuous one-parameter family of polyhedra,  $\mathcal{P}_t$ ,  $0 \leq t \leq 1$ , the following three conditions hold: (1)  $\mathcal{P}_0 = \mathcal{P}$ ; (2) each  $\mathcal{P}_t$  is isometric to  $\mathcal{P}_0$ ; (3) some  $\mathcal{P}_t$  is not congruent to  $\mathcal{P}_0$ .

Let  $K$  be defined as follows:  $K$  has vertices  $v_0, v_1, \dots, v_n, v_{n+1}$ , where  $v_1, \dots, v_n$  form a cycle ( $v_j$  adjacent to  $v_{j+1}$ ,  $j = 1, \dots, n - 1$  and  $v_n$  adjacent to  $v_1$ ) and  $v_0$  and  $v_{n+1}$  are each adjacent to all of  $v_1, \dots, v_n$ . Call  $\mathcal{P}(v_0) = N$  the north pole and  $\mathcal{P}(v_{n+1}) = S$  the south pole and  $\mathcal{P}(v_j) = p_j$ ,  $j = 1, \dots, n$ , vertices of the *equator*. Such a  $\mathcal{P}$  is called a *suspension*, see Figure 1.

**The variables and the fundamental equation.** Let  $\mathcal{P} : K \rightarrow \mathbb{R}^3$  be a suspension;  $N$  and  $S$  be the north and south poles of  $\mathcal{P}$ ; and  $p_1, p, \dots, p_n$  be the vertices on the equator in cyclic order, see Figure 1.

Below, we use the sign  $\stackrel{\text{def}}{=}$  as an abbreviation of the phrase ‘by definition’.

$$\begin{aligned}
 e_j &\stackrel{\text{def}}{=} N - p_j, & e'_j &\stackrel{\text{def}}{=} p_j - S, & j &= 1, 2, \dots, n, \\
 e_{n+1} &\stackrel{\text{def}}{=} e_1, & e'_{n+1} &\stackrel{\text{def}}{=} e'_1, \\
 e_{j,j+1} &\stackrel{\text{def}}{=} e_j - e_{j+1} = e'_{j+1} - e'_j & \text{are edges of the equator,} \\
 R &\stackrel{\text{def}}{=} e_j + e'_j = N - S, & x &\stackrel{\text{def}}{=} R \cdot R,
 \end{aligned}$$

where  $\cdot$  stands for the inner product in  $\mathbb{R}^3$ .

It is easy to see that if a suspension is flexible then  $x$ , the squared distance between the north and south poles, is non-constant. In the sequel, we treat

---

<sup>2</sup> In [2], the Strong Bellows Conjecture is proved for all Bricard’s flexible octahedra.

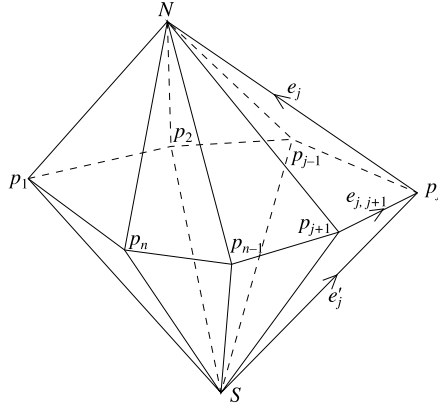


FIGURE 1. A suspension.

$x$  as an independent variable and consider all other expressions as functions of  $x$ .

Let  $\pi : \mathbb{R}^3 \rightarrow \pi(\mathbb{R}^3)$  be the orthogonal projection onto the plane perpendicular to  $R$  which is regarded as the plane of complex numbers. Using standard facts from analytic geometry and provided  $\pi(e_j) \neq 0$  for all  $j = 1, 2, \dots, n$ , we express the angle  $\theta_{j,j+1}$  from  $\pi(e_j)$  to  $\pi(e_{j+1})$  in  $\pi(\mathbb{R}^3)$  by the formula

$$e^{i\theta_{j,j+1}} = \frac{\pi(e_j)}{|\pi(e_j)|} \cdot \frac{\pi(e_{j+1})}{|\pi(e_{j+1})|} = \frac{G_{j,j+1}}{H_j H_{j+1}} \stackrel{\text{def}}{=} F_{j,j+1}, \quad j = 1, 2, \dots, n,$$

where

$$G_{j,j+1} \stackrel{\text{def}}{=} x(e_j \cdot e_{j+1}) - z_j z_{j+1} + y_{j,j+1}, \quad H_j \stackrel{\text{def}}{=} |R \times e_j|, \\ z_j \stackrel{\text{def}}{=} R \cdot e_j, \quad y_{j,j+1} \stackrel{\text{def}}{=} i|R|(e_j \times e_{j+1}) \cdot R.$$

Here,  $e_j \times e_{j+1}$  denotes the vector product and  $i \in \mathbb{C}$  is the imaginary unit,  $i^2 = -1$ .

Now the *fundamental flexing equation* derived in [7] is

$$(2.1) \quad \prod_{j=1}^n F_{j,j+1} = 1.$$

In a sense, (2.1) says that the suspension stays closed up as  $x$  varies.

**The roots and branch points.** As it is shown in [7], using more analytic geometry, we can prove that

$$y_{j,j+1} = -y_{j+1,j}, \quad z_j = \frac{1}{2}(x + e_j \cdot e_j - e'_j \cdot e'_j), \\ G_{j,j+1} G_{j+1,j} = H_j^2 H_{j+1}^2, \quad H_j^2 = x(e_j \cdot e_j) - z_j^2 = -\frac{1}{4}(x - r'_j)(x - r_j),$$

where  $r_j \stackrel{\text{def}}{=} (|e_j| + |e'_j|)^2$  and  $r'_j \stackrel{\text{def}}{=} (|e_j| - |e'_j|)^2$  are the roots of  $H_j^2$ , and

$$\begin{aligned} y_{j,j+1}^2 &= -x \det \begin{pmatrix} e_j \cdot e_j & e_j \cdot e_{j+1} & z_j \\ e_j \cdot e_{j+1} & e_{j+1} \cdot e_{j+1} & z_{j+1} \\ z_j & z_{j+1} & x \end{pmatrix} \\ &= \frac{1}{4}(e_{j,j+1} \cdot e_{j,j+1})x(x - b'_{j,j+1})(x - b_{j,j+1}). \end{aligned}$$

Here  $b_{j,j+1}, b'_{j,j+1}$  are the *branch points* of  $y_{j,j+1}^2$ . They can be described as the maximum and minimum value of  $x = |R|^2$  for the two triangles determined by  $e_j, e_{j+1}$  and  $e'_j, e'_{j+1}$  which share the common edge  $e_{j,j+1} = e_j - e_{j+1}$ . Namely, when  $x = b_{j,j+1}$  the two triangles are planar with  $N, S$  in the plane on opposite sides of the line determined by  $e_{j,j+1}$ . Similarly, when  $x = b'_{j,j+1}$ ,  $N, S$  are on the same side of the line. In particular,  $b'_{j,j+1}, b_{j,j+1}$  are real, nonnegative, and

$$0 \leq r'_j \leq b'_{j,j+1} \leq b_{j,j+1} \leq r_j.$$

We say  $y_{j,j+1}$  is *equivalent* to  $y_{k,k+1}$  or that  $j$  is equivalent to  $k$  if  $b'_{j,j+1} = b'_{k,k+1}$  and  $b_{j,j+1} = b_{k,k+1}$ .

Now we define  $\varepsilon_{j,j+1}$  as the sign of  $(e_j \times e_{j+1}) \cdot R$ . Note that  $\varepsilon_{j,j+1}$  is also the sign of  $\theta_{j,j+1}$ , and if the orientation of the suspension is chosen correctly  $\varepsilon_{j,j+1}$  is  $+1$  or  $-1$  as the suspension is locally convex or concave, respectively, at  $e_{j,j+1}$ . In any case, when  $x$  is in the flexing interval

$$y_{j,j+1} = \frac{i}{2} \varepsilon_{j,j+1} |e_{j,j+1}| \sqrt{-x(x - b'_{j,j+1})(x - b_{j,j+1})},$$

where the positive square root is chosen.

In [7] it is shown that, studying (2.1) near the branch points  $b'_{j,j+1}$  and  $b_{j,j+1}$ , we can split (2.1) into several equations, each corresponding to some equivalent class of  $j$ 's as described in the following lemma.

LEMMA. *Let  $\mathcal{P}$  be a suspension that flexes with variable  $x$ , and let  $\mathcal{C}_0 \subset \{1, 2, \dots, n\}$  be a subset corresponding to an equivalence class described above. Then*

$$(2.2) \quad \prod_{j \in \mathcal{C}_0} (Q_{j,j+1} + y_{j,j+1}) \prod_{j \in \mathcal{C}_0} (Q_{j,j+1} - y_{j,j+1})$$

is an identity in  $x$ , where  $Q_{j,j+1} \stackrel{\text{def}}{=} x(e_j \cdot e_{j+1}) - z_j z_{j+1}$  (or equivalently  $Q_{j,j+1} + y_{j,j+1} = G_{j,j+1}$ ).

Note that if (2.2) holds for each equivalence class  $\mathcal{C}_0$  then (2.1) holds. Thus, if we can construct a suspension such that (2.2) holds for each  $\mathcal{C}_0$ , we will have a flexor.

In order to construct a flexible suspension, we have to choose edge lengths  $|e_j|$ ,  $|e'_j|$ , and  $|e_{j,j+1}|$  ( $j = 1, 2, \dots, n$ ) such that equation (2.1) (or equation (2.2) for every class  $\mathcal{C}_0$ ) is an identity in  $x$ . As it was mentioned above,

$$(2.3) \quad \begin{aligned} & (Q_{j,j+1} + y_{j,j+1})(Q_{j,j+1} - y_{j,j+1}) \\ &= G_{j,j+1}G_{j+1,j} = H_j^2 H_{j+1}^2 \\ &= \frac{1}{16}(x - r'_j)(x - r_j)(x - r'_{j+1})(x - r_{j+1}) \end{aligned}$$

and the four roots in (2.3) are entirely arbitrary up to the conditions imposed on them that all the  $r'_j$ 's be smaller than the smallest  $r_j$ . Also it is easy to see that the four roots of (2.3) determine  $|e_j|$  and  $|e'_j|$  (but one does not know the order) by

$$\{|e_j|, |e'_j|\} = \left\{ \frac{1}{2}(\sqrt{r_j} + \sqrt{r'_j}), \frac{1}{2}(\sqrt{r_j} - \sqrt{r'_j}) \right\}.$$

The other parameters used to define the factors on the left of (2.3) are  $b_{j,j+1}$  and  $b'_{j,j+1}$ , and implicitly we shall discuss their relationship to the  $r_j$ 's later.

We now consider a fixed  $\mathcal{C}_0$ , with some  $b'$ ,  $b$ , and define

$$y = i\sqrt{-x(x - b')(x - b)}$$

so that

$$(2.4) \quad y^2 = x(x - b')(x - b).$$

The roots of  $G_{j,j+1}$  (i.e., of  $Q_{j,j+1} + y_{j,j+1}$ ) are the intersections of the curve defined by (2.4) and the quadratic

$$(2.5) \quad y = \frac{2Q_{j,j+1}(x)}{\varepsilon_{j,j+1}|e_{j,j+1}|}.$$

### Angle sign edge length lemmas.

LEMMA ([7, Lemmas 3 and 4]). *Let  $\mathcal{P}$  be a flexible suspension and let  $\mathcal{C}_0$  be an equivalence class of  $y_{j,j+1}$ 's. Then*

$$(2.6) \quad \sum_{j \in \mathcal{C}_0} \varepsilon_{j,j+1}|e_{j,j+1}| = 0$$

and

$$(2.7) \quad \sum_{j \in \mathcal{C}_0} y_{j,j+1} = 0.$$

Note that in [7] it is proven that (2.7) implies that the oriented volume of a flexible suspension identically equals zero during a flex and, thus, every embedded suspension is not flexible.

**The symmetry of the roots.** Note  $y_{j,j+1} = \frac{1}{2}\varepsilon_{j,j+1}|e_{j,j+1}|y$ . Thus, we may regard both sides of (2.2) as polynomials in  $x$  and  $y$  and a root as a pair  $(x, y)$ . Then (2.2) simply says that  $(x_0, y_0)$  is a root of the left side say, if and only if  $(x_0, -y_0)$  is also a root. This in turn says that the intersections defined by the curve (2.4) and all the curves defined by (2.5) are symmetric about the  $x$ -axis. Also it is not hard to see that if we have quadratics defined by (2.5) and the intersections are symmetric about the  $x$ -axis, then (2.2) holds.

One may be tempted into guessing that the symmetry condition implies that the quadratic factors of (2.2) cancel, but in fact this does not necessarily happen.

**The non-singular cubic.** We now come to the problem of how to describe in reasonably general terms how one creates factors with the symmetry condition of above.

The non-singular cubic, of which (2.2) is an example, is an Abelian variety. It turns out that it is possible to define a group operation on the curve in very natural way. Namely, we can choose any point and call it 0. We shall choose 0 to be the point at  $\infty$  on the  $y$ -axis. Then if  $Q_1, Q_2, Q_3$  are three distinct points on the intersection of a line with the curve, or two of the  $Q_j$ 's are equal and the line is tangent to the curve there, the group is defined by the condition  $Q_1 + Q_2 + Q_3 = 0$ . If  $Q$  is on the curve,  $-Q$  is the reflection of  $Q$  about the  $x$ -axis, see Figure 2. It is well known that this in fact defines an Abelian group [17].

**The quadratic.** Our basic problem is to describe how unsymmetric quadratics can intersect the cubic (2.4) in such a way that the intersections *are* symmetric.

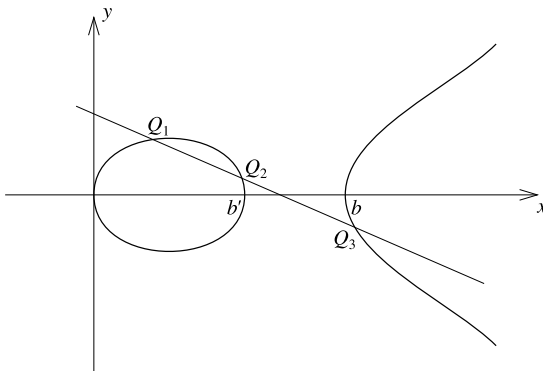


FIGURE 2. Definition of a group operation on a non-singular cubic.

Let  $y = \widehat{Q}(x)$  be a quadratic curve, where  $\widehat{Q}(x)$  is a quadratic function of  $x$ . It is easy to see that this curve intersects (2.4) at four finite points (perhaps complex points in general, but in our case they are always real). It is also easy to see that if we homogenize the equations (complete everything to projective situation) that there is in fact a double root at  $\infty$  (what we called the origin before) thus giving with Bezout's theorem. Let  $Q_1, Q_2, Q_3, Q_4$  be the four finite intersections of  $y = \widehat{Q}(x)$  with (2.4). Then by well-known results of algebraic geometry (e.g., Theorem 9.2 of [17]), we see that  $Q_1 + Q_2 + Q_3 + Q_4 = 0$ , and this condition is sufficient for the existence of such a  $y = \widehat{Q}(x)$  to intersect (2.4) at the four given points.

**The conditions.** We wish to write down a collection of conditions that must be satisfied if a suspension is to flex (with variable  $x$ ). However, we need a certain amount of notation. Let

$$\widehat{Q}(x) = \frac{2Q_{j,j+1}(x)}{\varepsilon_{j,j+1}|e_{j,j+1}|}$$

be the quadratic of (2.5). We have the four roots of (2.3) which serve as the intersection of (2.4) and (2.5), and we need a way of labeling them.

We label the four points  $(x, y)$  on the curve (2.4)  $Q'_{j-}, Q_{j-}, Q'_{j+1+}, Q_{j+1+}$  corresponding respectively to the  $x$ -values  $r'_j, r_j, r'_{j+1}, r_{j+1}$ . Also for each point  $Q$  on the curve (2.4) let  $\overline{Q}$  denote its  $x$  coordinate.

If the  $Q_{j\pm}$ 's correspond to the roots of (2.2), they must satisfy the following conditions.

- (A)  $\overline{Q'_{j-}} = \overline{Q'_{j+}}, \overline{Q_{j-}} = \overline{Q_{j+}}$ , for all  $j = 1, 2, \dots, n$ .
- (B)  $Q'_{j-} + Q_{j-} + Q'_{j+1+} + Q_{j+1+} = 0$  in the group corresponding to  $j \in \mathcal{C}_0$ .
- (C) For every equivalence class  $\mathcal{C}_0$ , the collection of  $Q$ 's (counting multiplicities) is symmetric about the  $x$ -axis. (Also, the  $Q'$ 's are on the finite component and the  $Q$ 's on the infinite component.)

(B) and (C) have been discussed above. (A) is simply the condition that  $r_j$  and  $r'_j$  depend only on  $|e_j|$  and  $|e'_j|$ . Also it is handy to note that if  $j$  and  $j+1$  are in the same equivalence class (thus, defining the same curve (2.4) and the same group), then (A) is just the condition that  $Q'_{j-} = \pm Q'_{j+}, Q_{j-} = \pm Q_{j+}$ .

Using the conditions (A), (B), (C) it is possible to write down the points on a curve (2.4) that would hopefully come from a non-trivial flexor.

**The flow graph.** The conditions above are sufficient to enable one to create many non-trivial flexors. In this subsection we describe a *flow graph* associated to a non-trivial flexor which considerably simplifies the construction of points which satisfy the conditions (A), (B), (C).

We construct a graph,  $G_{\mathcal{C}_0}$  (a multi-graph in the sense of F. Harary [11]), corresponding to each equivalence class or group as follows: The vertices of  $G_{\mathcal{C}_0}$  consist of the elements  $j \in \mathcal{C}_0$ . By property (C), there is a pairing between

the roots, the  $Q_{j\pm}$ 's and  $Q'_{j\pm}$ 's. Choose one such pairing. We say  $j$  is *adjacent* to  $k$  if one of the  $Q$ 's for  $j$ ,  $Q'_{j-}$ ,  $Q_{j-}$ ,  $Q'_{j+1+}$ ,  $Q_{j+1+}$ , is paired with minus (in the group) one of the  $Q$ 's for  $k$ .

We furthermore wish to define a *flow* on  $G_{C_0}$  in the nature described in [4]. Assign a direction to the edges of  $G_{C_0}$  arbitrarily. If the direction of an edge is from  $j$  to  $k$ , then the flow is  $X$ , if  $X$  is the value (thought of as in the group) of the  $j$   $Q$  that is paired with  $k$ . Note that condition (B) implies that the total flow into any vertex is zero.

Since each  $j$  corresponds to four  $Q$ 's, the degree (not counting direction) at each vertex is four. Notice, also, from the nature of the graph and the fact that (2.4) has two components each  $Q'$  is necessarily paired with a  $Q'$  and similarly for the  $Q$ 's. This is because the  $Q'$ 's are all on the finite component of the cubic. Thus, the edges can be partitioned into two equal collections, corresponding to the  $Q'$ 's and the  $Q$ 's, and each vertex is adjacent to two edges of each type. Each collection of edges is called a *two-factor* and we call them  $F'$  and  $F$ . Thus, the graph obtained is simply a graph with two disjoint two-factors, that also has a non-trivial flow.

**An example.** Consider the flow graph which represents the associated graph with double lines being the  $F'$  factors, and single lines being the  $F$  factors. The flow graph shown on Figure 3 generates Table 1.

Note that condition (A) puts additional constraints on the flow and is automatically incorporated in the above flows.

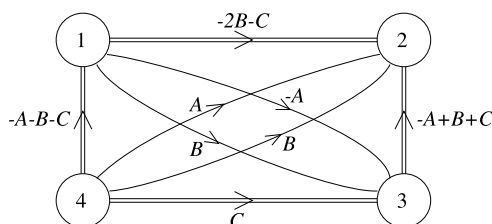


FIGURE 3. An example of a flow graph.

TABLE 1. Points on the cubic that correspond to the flow graph shown on Figure 3

| $j$ | $Q_{j-1,-}$ | $Q_{j+}$ | $Q'_{j-1,-}$ | $Q'_{j+}$    |
|-----|-------------|----------|--------------|--------------|
| 1   | $A$         | $B$      | $C$          | $-A - B - C$ |
| 2   | $B$         | $-A$     | $A + B + C$  | $-2B - C$    |
| 3   | $-A$        | $-B$     | $2B + C$     | $A - B - C$  |
| 4   | $-B$        | $A$      | $-A + B + C$ | $-C$         |

Table 1 corresponds to the first type flexible octahedra, which are constructed by taking a quadrilateral in the plane that has opposite edges equal, but crosses itself, and then choosing the north and south pole in the plane of symmetry through the crossing point, see Figure 4. These were described, e.g., in [14].

### 3. A flexible suspension with a hexagonal equator

In this section, we construct a flexible suspension with a hexagonal equator.

**Step 1: Choosing the flow graph.** Consider the directed multigraph shown on Figure 5. Suppose the flows corresponding to the double lines are called  $F'$  factors and the flows corresponding to the single lines are called  $F$  factors.

Note that this graph satisfies the conditions (A), (B), and (C) mentioned in Section 2.

**Step 2: Calculating the table.** Consider Table 2.

Note that that Table 2 corresponds to (or is generated by) the flow graph shown on Figure 5.

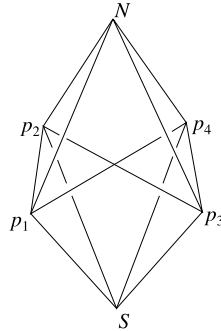


FIGURE 4. Bricard's flexible octahedron of the first type.

TABLE 2. Points on the cubic that correspond to the flow graph shown on Figure 5

| $j$ | $Q_{j-1,-}$       | $Q_{j+}$          | $Q'_{j-1,-}$ | $Q'_{j+}$ |
|-----|-------------------|-------------------|--------------|-----------|
| 1   | $C$               | $-A + B - C$      | $A$          | $-B$      |
| 2   | $A - B + C$       | $-A + 2B - C - D$ | $-B$         | $D$       |
| 3   | $A - 2B + C + D$  | $2B - C - 2D$     | $D$          | $-A$      |
| 4   | $-2B + C + 2D$    | $A + B - C - 2D$  | $-A$         | $B$       |
| 5   | $-A - B + C + 2D$ | $A - C - D$       | $B$          | $-D$      |
| 6   | $-A + C + D$      | $-C$              | $-D$         | $A$       |

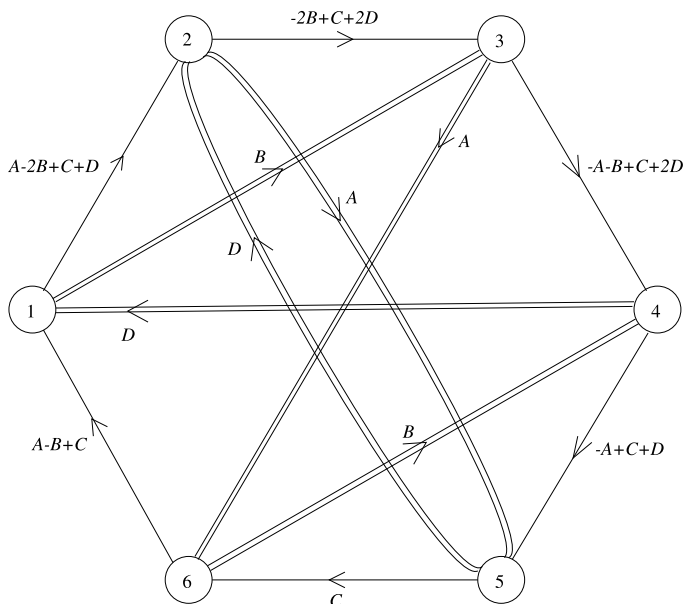


FIGURE 5. Flow graph of a flexible suspension with a hexagonal equator.

Our goal is to construct a flexible suspension with the unique equivalence class  $\mathcal{C}$  and with the table shown in Table 2.

**Step 3: Calculating the points on the cubic.** We fix  $b' = 51$ ,  $b = 100$  and consider  $y$  as an algebraic function of  $x$  determined by the equation

$$(3.1) \quad y^2 = x(x - b')(x - b),$$

see Figure 6. By definition, we put

$$(3.2) \quad \begin{aligned} A &= (2, 98); & B &= \left( \frac{4039540}{762129}, \frac{100768585960}{665338617} \right); \\ C &= (102, -102); & D &= (30, -210). \end{aligned}$$

Obviously, points  $A$ ,  $B$ , and  $D$  lie on the bounded component of non-singular cubic (3.1) while point  $C$  lies on the unbounded component, as it is shown on Figure 6.

Using either the definition of the group addition on non-singular cubic (3.1) given above in Section 2 or an explicit formula for the group addition derived

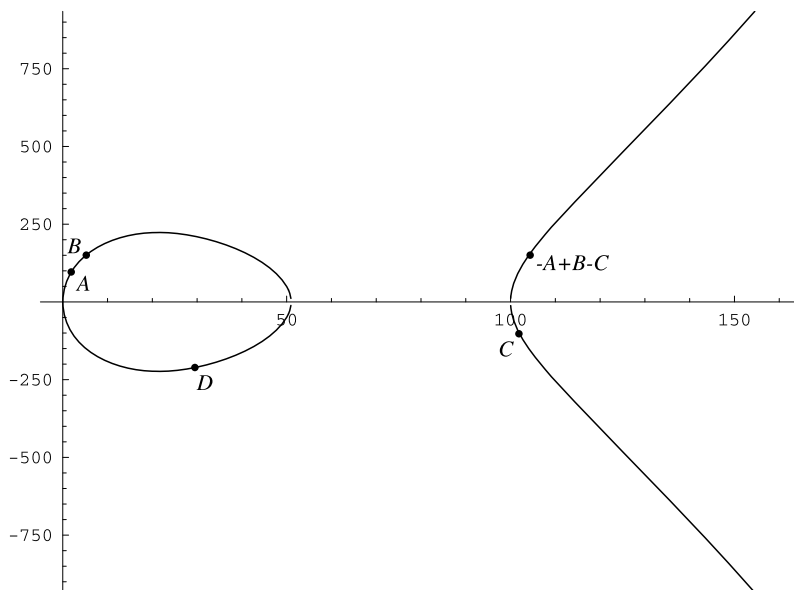


FIGURE 6. Plot of non-singular cubic (3.1).

in [12] with the help of the Weierstrass function, we write the coordinates of the sum of the points  $(u_1, v_1)$  and  $(u_2, v_2)$  on the cubic as follows

$$(3.3) \quad (u_1, v_1) + (u_2, v_2) = \left( b' + b - u_1 - u_2 + \left( \frac{v_1 - v_2}{u_1 - u_2} \right)^2, \right. \\ \left. v_1 - \frac{v_1 - v_2}{u_1 - u_2} \left[ b' + b - 2u_1 - u_2 + \left( \frac{v_1 - v_2}{u_1 - u_2} \right)^2 \right] \right).$$

Using formula (3.3) and the system of analytic computations *Mathematica*, we calculate coordinates of the other points mentioned in Table 2<sup>3</sup>

$$(3.4) \quad \begin{aligned} -A + B - C &= \left( \frac{30931440}{292681}, \frac{28695544920}{158340421} \right); \\ -A + 2B - C - D &= \left( \frac{5661629280833549058327770}{3946395061554216239809}, \right. \\ &\quad \left. \frac{12760353764630956864568385268955559830}{24791387777118200103588255865377} \right); \end{aligned}$$

<sup>3</sup> According to Section 2, if point  $X$  has coordinates  $(u, v)$  then point  $-X$  has coordinates  $(u, -v)$  and, thus, can be easily found. This is the reason why we write in (3.4) and show on Figure 6 only one of the points  $X$  and  $-X$ .

$$\begin{aligned}
 2B - C - 2D &= \left( \frac{98365674940749318}{521862179555809}, \right. \\
 &\quad \left. - \frac{18053411514039795685625754}{11921577754013306206127} \right); \\
 A + B - C - 2D &= (240, -2520); \\
 A - C - D &= \left( \frac{49130}{121}, \frac{8840510}{1331} \right).
 \end{aligned}$$

Point  $-A + B - C$  is also shown on Figure 6, while the other points are too far from the origin to be shown there.

**Step 4: Calculating the  $r'_j$ 's,  $r_j$ 's, and  $\varepsilon_{j,j+1}$ 's.** Recall that in Section 2, we label the points  $Q'_{j-}$  and  $Q_{j-}$  on the curve (2.4) in such a way that their  $x$ -values are  $r'_j$  and  $r_j$  respectively. Thus, Table 2 and formulas (3.2) and (3.3) immediately give us the following values for the  $r'_j$ 's and  $r_j$ 's in Table 3.

Note that, using formulas (3.2) and (3.4), we can read from the appropriate line in Table 2 all coordinates of the four points of intersection of cubic (3.1) and the quadratic (2.5), i.e.,

$$y = \frac{2Q_{j,j+1}(x)}{\varepsilon_{j,j+1}|e_{j,j+1}|}.$$

Hence, the branches of (2.5) are oriented upward if and only if the  $y$ -coordinate of the right-most of the four points of intersection is positive. Now, taking into account that the leading coefficient of  $Q_{j,j+1}(x)$  equals  $-1/4$ , we decide whether  $\varepsilon_{j,j+1} = +1$  or  $\varepsilon_{j,j+1} = -1$ .

For example,

$$\begin{aligned}
 Q'_1 &= -B \left( \frac{4039540}{762129}, -\frac{100768585960}{665338617} \right) \approx (5.30, -151.45), \\
 Q'_2 &= D(30, -210),
 \end{aligned}$$

TABLE 3. Results of the symbolic and numerical calculations of the  $r'_j$ 's,  $r_j$ 's, and  $\varepsilon_{j,j+1}$ 's

| $j$ | $r'_j$                                | $r_j$  | $\varepsilon_{j,j+1}$ |
|-----|---------------------------------------|--|-----------------------|
| 1   | $\frac{4039540}{762129} \approx 5.30$ | $\frac{30931440}{292681} \approx 105.68$                                   | -1                    |
| 2   | 30                                    | $\frac{5661629280833549058327770}{3946395061554216239809} \approx 1434.63$ | +1                    |
| 3   | 2                                     | $\frac{98365674940749318}{521862179555809} \approx 188.49$                 | +1                    |
| 4   | $\frac{4039540}{762129} \approx 5.30$ | 240  | -1                    |
| 5   | 30                                    | $\frac{49130}{121} \approx 406.03$   | +1                    |
| 6   | 2                                     | 102  | -1                    |

$$Q_1 = A - B + C \left( \frac{30931440}{292681}, -\frac{28695544920}{158340421} \right) \approx (105.68, -181.23),$$

$$Q_2 = -A + 2B - C - D \left( \frac{5661629280833549058327770}{3946395061554216239809}, \frac{12760353764630956864568385268955559830}{24791387777118200103588255865377} \right) \approx (1434.63, 51470.90).$$

The right-most point is  $Q_2$  and its  $y$ -coordinate is positive. Hence, the leading coefficient of quadratic (2.5) is positive and  $\varepsilon_{1,2} = -1$ .

Proceeding in the same way, we find  $\varepsilon_{j,j+1}$  for  $j = 2, \dots, 6$  and put the results on Table 3.

**Step 5: Calculating the  $|e'_j|$ 's,  $|e_j|$ 's, and  $|e_{ij}|$ 's.** Recall from Section 2 that the lengths of the edges of the suspension adjacent to the north and south poles,  $|e_j|$  and  $|e'_j|$  respectively, are such that

$$(3.5) \quad \{|e_j|, |e'_j|\} = \left\{ \frac{1}{2} \left( \sqrt{r_j} + \sqrt{r'_j} \right), \frac{1}{2} \left( \sqrt{r_j} - \sqrt{r'_j} \right) \right\}.$$

Note that this relation does not allow us to determine  $|e_j|$  and  $|e'_j|$  precisely because we do not know the order.

Let us call the union of triangles  $\langle N, p_j, p_{j+1} \rangle$  and  $\langle S, p_j, p_{j+1} \rangle$  the  $j$ -sector of the suspension. Obviously, every  $j$ -sector has two flat positions. In one flat position, the both triangles lie on the same side of the line determined by the equator edge  $\langle p_j, p_{j+1} \rangle$  while in the other flat position the triangles lie on the different sides of that line. Using the notation  $e_j^- = \min\{|e'_j|, |e_j|\}$  and  $e_j^+ = \max\{|e'_j|, |e_j|\}$ , we draw the four possible cases of the relative location of the triangles  $\langle N, p_j, p_{j+1} \rangle$  and  $\langle S, p_j, p_{j+1} \rangle$  on Figure 7. The four cases shown in Figure 7 correspond to the situation when  $|e_j| = e_j^+$ . The other four cases, corresponding to the situation when  $|e_j| = e_j^-$ , can be drawn similarly. We do not draw those four cases because they can be obtained from the cases shown on Figure 7 by interchanging the north and south poles, i.e., by replacing  $S$  by  $N$  and  $N$  by  $S$  on Figure 7.

Consider Case I shown on Figure 7. Observe that the same sector has yet another flat position which may be obtained by rotating triangle  $\langle N, p_j, p_{j+1} \rangle$  around its side  $\langle p_j, p_{j+1} \rangle$  in 3-space to the angle  $\pi$ . The result is shown on Figure 8. Now triangles  $\langle N, p_j, p_{j+1} \rangle$  and  $\langle S, p_j, p_{j+1} \rangle$  lie on one side of the line through vertices  $p_j$  and  $p_{j+1}$ . We say that the configuration shown on Figure 8 is obtained from Case I on Figure 7 by a *flip*. Similarly, we may apply a flip to each of the Cases II–IV shown on Figure 7.

For every sector we know from Section 2 that, in one flat position, the distance between the north and south poles,  $N$  and  $S$ , equals  $b$ , while in the other flat position it is equal to  $b'$ . At the very beginning of Section 3, we have fixed  $b' = 51$  and  $b = 100$ .

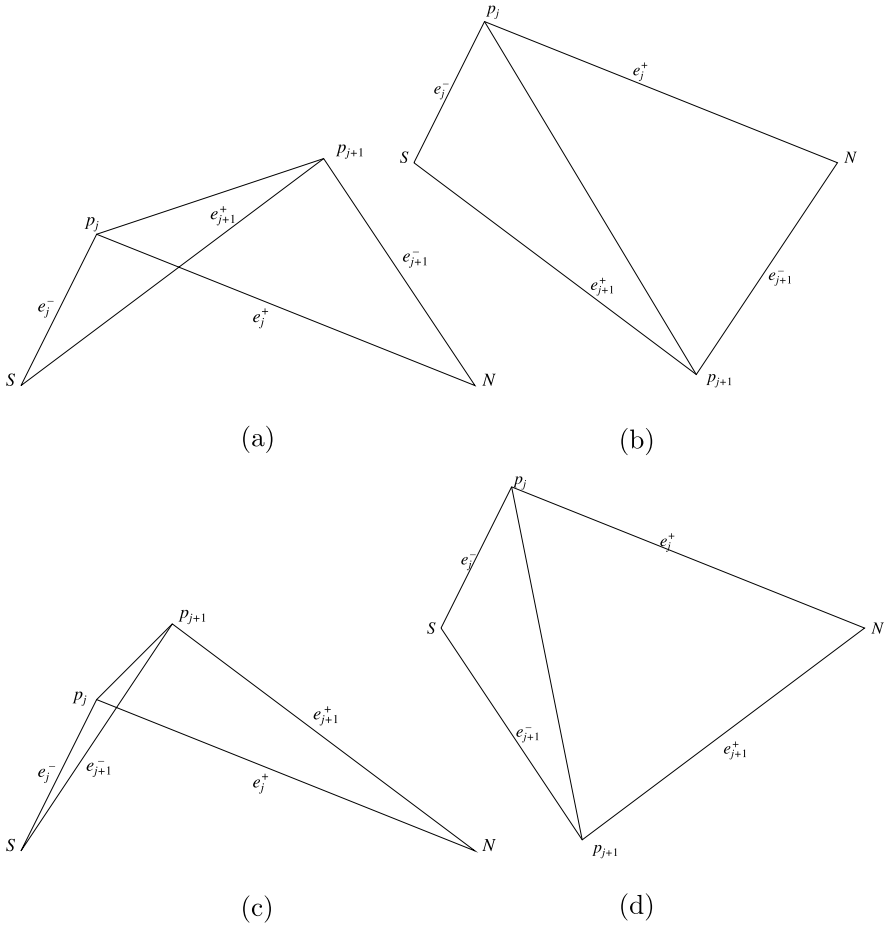


FIGURE 7. Four cases of the relative location of triangles  $\langle N, p_j, p_{j+1} \rangle$  and  $\langle S, p_j, p_{j+1} \rangle$  provided that  $|e_j| = e_j^+$ : (a) Case I:  $|e_{j+1}| = e_{j+1}^-$  and triangles lie on one side of the line  $p_j p_{j+1}$ . (b) Case II:  $|e_{j+1}| = e_{j+1}^-$  and triangles lie on different sides of the line  $p_j p_{j+1}$ . (c) Case III:  $|e_{j+1}| = e_{j+1}^+$  and triangles lie on one side of the line  $p_j p_{j+1}$ . (d) Case IV:  $|e_{j+1}| = e_{j+1}^+$  and triangles lie on different sides of the line  $p_j p_{j+1}$ .

For each  $j = 1, \dots, 6$ , we use Table 3 to compute

$$e_j^- = \min \left\{ \frac{1}{2} \left( \sqrt{r_j} + \sqrt{r'_j} \right), \frac{1}{2} \left( \sqrt{r_j} - \sqrt{r'_j} \right) \right\}$$

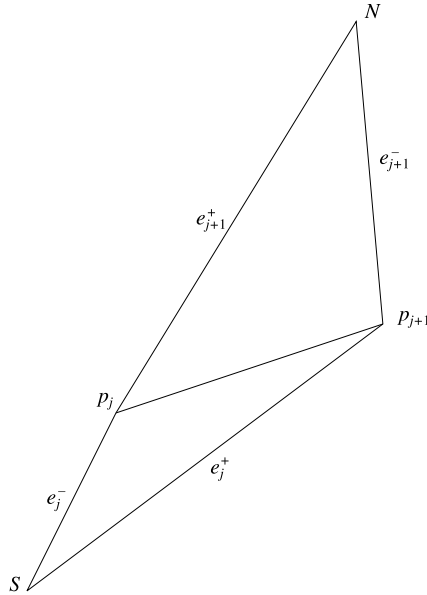


FIGURE 8. The result of a flip applied to triangles  $\langle N, p_j, p_{j+1} \rangle$  and  $\langle S, p_j, p_{j+1} \rangle$  shown on Figure 7(a).

and

$$e_j^+ = \max \left\{ \frac{1}{2} \left( \sqrt{r_j} + \sqrt{r'_j} \right), \frac{1}{2} \left( \sqrt{r_j} - \sqrt{r'_j} \right) \right\}.$$

Then, for each of the Cases I–IV, we put the poles,  $S$  and  $N$ , at the points  $(0, 0)$  and  $(10, 0)$ <sup>4</sup>, respectively and calculate the coordinates of the points  $p_j$  and  $p_{j+1}$ . The distance  $|p_j - p_{j+1}|$  is a candidate for the length  $e_{j,j+1}$  of the equatorial edge. At last, we calculate the coordinates of the north pole under the flip transformation (i.e., under the reflection of triangle  $\langle N, p_j, p_{j+1} \rangle$  with respect to the line through the points  $p_j$  and  $p_{j+1}$ ) and if this distance equals exactly  $\sqrt{51}$  (i.e., this distance squared equals  $b' = 51$  that is the square of the minimal distance between the poles during the flex) then we say that the choice for the  $e_j, e'_j, e_{j+1}, e'_{j+1},$  and  $e_{j,j+1}$  is correct. Note that, when we calculate  $e_j, e'_j, e_{j+1}, e'_{j+1},$  and  $e_{j,j+1}$  for the first sector we can obviously interchange the north and south poles, but as soon as the poles,  $N$  and  $S$ , are fixed for the first sector, the above described procedure determine the edge lengths in a unique way. We accumulate the results of such calculations in Tables 4 and 5.

---

<sup>4</sup> Recall from Section 2 that  $b = 100$  is the square of the maximal distance between the poles during the flex.

TABLE 4. Results of the symbolic and numerical calculations of the  $|e_j|$ 's and  $|e'_j|$ 's

| $j$ | $ e_j $   | $ e'_j $  |
|-----|---|---|
| 1   | $\frac{1}{2}(\frac{1436\sqrt{15}}{541} + \frac{218\sqrt{85}}{873}) \approx 6.29$    | $\frac{1}{2}(\frac{1436\sqrt{15}}{541} - \frac{218\sqrt{85}}{873}) \approx 3.99$    |
| 2   | $\frac{1}{2}(\frac{182493018091\sqrt{170}}{62820339553} - \sqrt{30}) \approx 16.20$ | $\frac{1}{2}(\frac{182493018091\sqrt{170}}{62820339553} + \sqrt{30}) \approx 21.68$ |
| 3   | $\frac{1}{2}(\frac{31054297\sqrt{102}}{22844303} - \sqrt{2}) \approx 6.16$          | $\frac{1}{2}(\frac{31054297\sqrt{102}}{22844303} + \sqrt{2}) \approx 7.57$          |
| 4   | $\frac{1}{2}(4\sqrt{15} - \frac{218\sqrt{85}}{873}) \approx 6.59$                   | $\frac{1}{2}(4\sqrt{15} + \frac{218\sqrt{85}}{873}) \approx 8.90$                   |
| 5   | $\frac{1}{2}(\frac{17\sqrt{170}}{11} - \sqrt{30}) \approx 7.34$                     | $\frac{1}{2}(\frac{17\sqrt{170}}{11} + \sqrt{30}) \approx 12.81$                    |
| 6   | $\frac{1}{2}(\sqrt{102} + \sqrt{2}) \approx 5.76$                                   | $\frac{1}{2}(\sqrt{102} - \sqrt{2}) \approx 4.34$                                   |

TABLE 5. Results of the symbolic and numerical calculations of the  $|e_{j,j+1}|$ 's

| $j$ | $ e_{j,j+1} $  |
|-----|--|
| 1   | $\frac{541419683182996345}{29669606628505029} \approx 18.25$     |
| 2   | $\frac{31635727886833754300}{1435086871311616559} \approx 22.04$ |
| 3   | $\frac{27288800741}{19943076519} \approx 1.37$                   |
| 4   | $\frac{130585}{9603} \approx 13.60$                              |
| 5   | $\frac{100}{11} \approx 9.09$                                    |
| 6   | $\frac{310327}{472293} \approx 0.66$                             |

Let us mention that when we calculate  $e_{61}$ , we additionally take into account that, at that moment, we already know the order how the edges  $e_1, e'_1, e_6$  and  $e'_6$  are attached to the north and south poles,  $N$  and  $S$  respectively, and, of course, their lengths which are shown in Table 4.

On Figure 9, we show how the next sector is glued to the previous one in a flat position corresponding to  $x = 100$ . To this end, we draw the last glued sector with thicken lines in contrast with all the preceding sectors. It is expected that, in each sector, the triangles  $\langle N, p_j, p_{j+1} \rangle$  and  $\langle S, p_j, p_{j+1} \rangle$  are located on different sides of the line through the points  $p_j$  and  $p_{j+1}$ .

Fix an orientation of the whole suspension constructed. By  $\varphi_j$  denote the dihedral angle of the suspension at the edge  $\langle N, p_j \rangle$  (for possibly singular suspensions the notion of a dihedral angle is clear as long as each face is embedded). Similarly, denote by  $\varphi'_j$  and  $\varphi_{j,j+1}$  the dihedral angles at the edges  $\langle S, p'_j \rangle$  and  $\langle p_j, p_{j+1} \rangle$ . Note that these angles are functions in  $x$ , the squared distance between the north and south poles,  $N$  and  $S$ . Obviously,

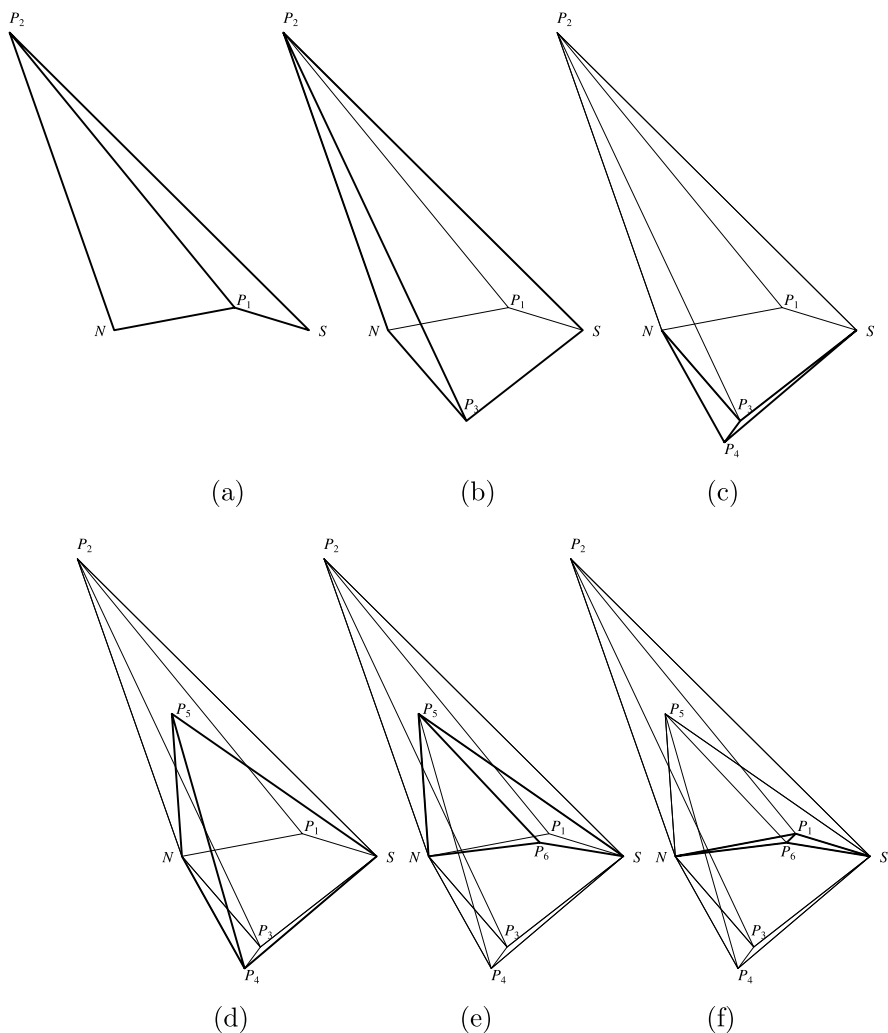


FIGURE 9. Step-by-step gluing of sectors of the suspension in a flat position corresponding to  $x = 100$ . On each step the last glued sector is shown with thickened lines. (a) 1-sector. (b) 1- and 2-sectors. (c) 1-, 2- and 3-sectors. (d) 1- to 4-sectors. (e) 1- to 5-sectors. (f) 1- to 6-sectors.

Figure 9 lets us find those angles modulo  $2\pi$  for  $x = 100$ . The results are presented in Table 6.

TABLE 6. Dihedral angles of the suspension in the two flat positions corresponding to  $x = 100$  and  $x = 51$

| $j$ | $\varphi_j(100)$ | $\varphi'_j(100)$ | $\varphi_{j,j+1}(100)$ | $\varphi_j(51)$ | $\varphi'_j(51)$ | $\varphi_{j,j+1}(51)$ |
|-----|------------------|-------------------|------------------------|-----------------|------------------|-----------------------|
| 1   | $\pi$            | $\pi$             | $\pi$                  | 0               | 0                | 0                     |
| 2   | 0                | 0                 | $\pi$                  | $\pi$           | $\pi$            | 0                     |
| 3   | $\pi$            | $\pi$             | $\pi$                  | 0               | 0                | 0                     |
| 4   | 0                | 0                 | $\pi$                  | $\pi$           | $\pi$            | 0                     |
| 5   | 0                | 0                 | $\pi$                  | $\pi$           | $\pi$            | 0                     |
| 6   | 0                | 0                 | $\pi$                  | $\pi$           | $\pi$            | 0                     |

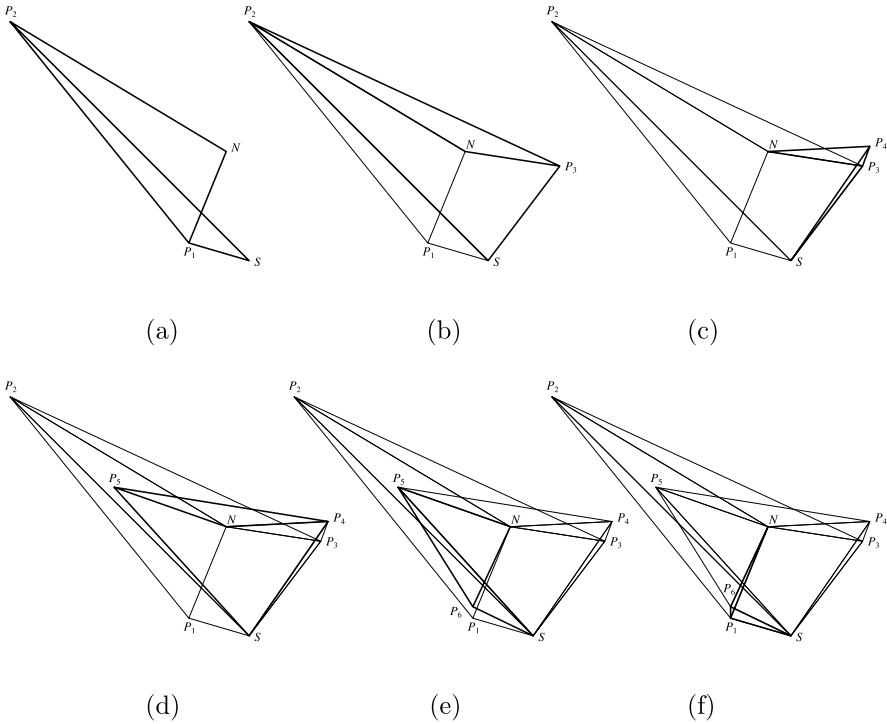


FIGURE 10. Step-by-step gluing of sectors of the suspension in a flat position corresponding to  $x = 51$ . On each step the last glued sector is shown with thickened lines. (a) 1-sector. (b) 1- and 2-sectors. (c) 1-, 2- and 3-sectors. (d) 1- to 4-sectors. (e) 1- to 5-sectors. (f) 1- to 6-sectors.

On Figure 10, we show how the next sector is glued to the previous one in a flat position corresponding to  $x = 51$ . As before we draw the last glued sector

with thick lines in contrast with all the preceding sectors. It is expected that, in each sector, the triangles  $\langle N, p_j, p_{j+1} \rangle$  and  $\langle S, p_j, p_{j+1} \rangle$  are located on the same side of the line through the points  $p_j$  and  $p_{j+1}$ .

Obviously, Figure 10 lets us find those angles modulo  $2\pi$  for  $x = 51$ . The results are presented in Table 6.

**Comparison with previously known theorems.** It follows from Mikhailev’s theorem [13] that if a suspension with an  $n$ -gon equator  $p_1, \dots, p_n$  is bent in such a way that the length of the ‘short’ diagonal  $\langle p_{j-1}, p_{j+1} \rangle$  is non-constant for some  $j = 1, \dots, n$  then there exists  $k = 1, \dots, n$ ,  $k \neq j \pm 1$ , such that

$$(3.6) \quad |e_j| + (-1)^{\sigma_1}|e'_j| + (-1)^{\sigma_2}|e_k| + (-1)^{\sigma_3}|e'_k| = 0$$

with some integers  $\sigma_1, \sigma_2, \sigma_3$ .

Note that (3.6) is satisfied for the above constructed suspension  $\mathcal{S}$  with a hexagonal equator, namely,

$$\begin{aligned} |e_1| - |e'_1| + |e_4| - |e'_4| &= 0, \\ |e_2| - |e'_2| - |e_5| + |e'_5| &= 0, \\ |e_3| - |e'_3| + |e_6| - |e'_6| &= 0. \end{aligned}$$

It follows from another theorem of Mikhailev [13] that, for every flexible suspension with an  $n$ -gon equator  $p_1, \dots, p_n$

$$(3.7) \quad \sum_{j=1}^n (-1)^{\sigma_j} |e_{j,j+1}| = 0$$

with some integers  $\sigma_j$ .

Note that (3.7) obviously follows from (2.6) while the latter was proven in [7] more than 25 years prior to Mikhailev’s paper [13]. Moreover, (2.6) provides us with additional geometric information that (3.7) holds with  $(-1)^{\sigma_j} = \varepsilon_{j,j+1}$ , where, as it was specified in Section 2,  $\varepsilon_{j,j+1}$  equals the sign of  $(e_j \times e_{j+1}) \cdot R$ .

Using data from Tables 3 and 5, we find by direct calculations that (3.7), or (2.6), is satisfied for the above constructed suspension  $\mathcal{S}$  with a hexagonal equator, namely,

$$(3.8) \quad -|e_{12}| + |e_{23}| + |e_{34}| - |e_{45}| + |e_{56}| - |e_{61}| = 0$$

or

$$\begin{aligned} & -\frac{541419683182996345}{29669606628505029} + \frac{31635727886833754300}{1435086871311616559} \\ & + \frac{27288800741}{19943076519} - \frac{130585}{9603} + \frac{100}{11} - \frac{310327}{472293} = 0. \end{aligned}$$

**Discussion.** Obviously, every flexible octahedron (known also as a Bricard octahedron) can be considered as a flexible suspension with a quadrilateral equator and gives rise to trivial flexible suspensions with, say, pentagonal or hexagonal equators which can be constructed as follows: fix an interior point on an equator edge and join it with the north and south poles with new edges (i.e., subdivide some faces of the octahedron).

There is another obvious way to construct a trivial flexible suspension with pentagonal or hexagonal equator: start with an arbitrary suspension with a pentagonal or hexagonal equator; remove the star of the south pole and treat the star of the north pole as a twice-covered polyhedral surface.

The above mentioned trivial flexible suspensions, definitely, cannot help us to construct a counterexample to the Strong Bellows Conjecture. We were not able to construct a non-trivial flexible suspension with pentagonal equator, but we can summarize the results of this section in the following theorem.

**THEOREM.** *The suspension  $\mathcal{S}$ , constructed above, provides us with a non-trivial example of a flexible suspension with a hexagonal equator.*

#### 4. An attack on the Strong Bellows Conjecture

In this section, we study properties of the flexible suspension with a hexagonal equator  $\mathcal{S}$  constructed in Section 3 which are related to the Strong Bellows Conjecture.

**Dehn invariants and the Strong Bellows Conjecture.** Let  $f : \mathbb{R} \rightarrow \mathbb{R}$  be a  $\mathbb{Q}$ -linear function such that  $f(\pi) = 0$ , i.e., let  $f(px + qy) = pf(x) + qf(y)$  for all  $p, q \in \mathbb{Q}$ ,  $x, y \in \mathbb{R}$  and  $f(\pi) = 0$ . The sum

$$D_f(\mathcal{P}) = \sum f(\varphi_j)\ell_j$$

is called the *Dehn invariant* of a possibly singular polyhedron  $\mathcal{P}$  in Euclidean 3-space. Here  $\varphi_j$  is the (internal) dihedral angle at the  $j$ 's edge,  $\ell_j$  is the length of the  $j$ 's edge, and the sum is taken over all the edges of  $\mathcal{P}$ .

It is well known that *two embedded polyhedra in Euclidean 3-space are scissors congruent if and only if they have the same volume and every Dehn invariant takes the same value for those polyhedra*, see [6] or [10].

It seems natural to have this theorem in mind when approaching the Strong Bellows Conjecture but the first problem here is that we should extend the notions of volume, internal dihedral angle, and Dehn invariant onto an arbitrary oriented polyhedron.

The extension of the notion of volume we need is the standard notion of the oriented volume [7]. In 1996, I. Kh. Sabitov [15] has proved that *every oriented flexible polyhedron in Euclidean 3-space preserves its oriented volume during a flex* and, thus, gave an affirmative answer to the Bellows Conjecture. An improved presentation is given in [16]; another proof is published in [9].

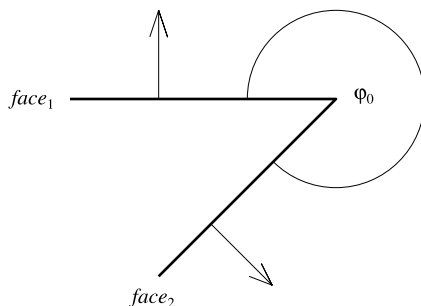


FIGURE 11. ‘Usual’ dihedral angle  $\varphi_0$  between two faces.

In order to define the Dehn invariant, we will assume that each face of the polyhedron is *non-degenerate*. This means that the three vertices of each triangle of the triangulation do not lie in a line. Alternatively, if the faces of the polyhedron are not all triangles, we assume that they are convex two-dimensional polygons and each edge of the polyhedron has non-zero length. In principle, we could try to define the Dehn invariant even in the degenerate case, but we do not need to do that here.

We define the *dihedral angle* at an edge  $\ell$  of an oriented polyhedron in Euclidean 3-space as a multi-valued function  $\varphi = \varphi_0 + 2\pi k$ , where  $k$  is an integer and one of the values,  $\varphi_0$ , is defined as the ‘usual’ dihedral angle between the two faces  $f_1$  and  $f_2$  adjacent to  $\ell$  measured from the side determined by the orientation. See Figure 11. In other words we can say that  $\varphi_0$  is a number between 0 and  $2\pi$  which is obtained as the product of  $2\pi$  and the proportion of a sufficiently small ball centered at a relative interior point of  $\ell$  which is contained in the intersection of the two half-spaces determined by oriented faces  $f_1$  and  $f_2$ .

As in complex analysis, we say that values of dihedral angle  $\varphi$  which correspond to different values of  $k$  represent different *branches* of that multi-valued function. For a flexible polyhedron, we fix a particular value (or a branch) of every dihedral angle (i.e., fix all  $k$ ’s) in a single position and assume that those particular values change continuously in the course of the flex. This means that the value of a dihedral angle may drift from one branch to another during the flex.

The sum

$$D_f(\mathcal{P}) = \sum f(\varphi_j)\ell_j$$

is called the *Dehn invariant* of an oriented (possibly singular) polyhedron  $\mathcal{P}$  in Euclidean 3-space. Here  $f : \mathbb{R} \rightarrow \mathbb{R}$  is a  $\mathbb{Q}$ -linear function such that  $f(\pi) = 0$ ,  $\varphi_j$  is the dihedral angle at the  $j$ ’s edge,  $\ell_j$  is the length of the  $j$ ’s

edge, and the sum is taken over all the edges of  $\mathcal{P}$ . Note that  $D_f$  does not depend on a choice of a branch of  $\varphi_j$ .

Now we can formulate the *Strong Bellows Conjecture: Every Dehn invariant of an oriented, possibly singular but, non-degenerate, flexible polyhedron in Euclidean 3-space remains constant during the flex.*

**An attack on the Strong Bellows Conjecture.** Let us treat  $\mathbb{R}$  as an (infinite-dimensional) vector space over  $\mathbb{Q}$ . It is known that, if Zermelo’s axiom is true, there exist a basis  $\mathfrak{H}$  in that vector space [6] (this means that every real number  $x$  is expressible uniquely in the form of a finite linear combination of elements of  $\mathfrak{H}$  with rational coefficients  $x = \alpha_1 e_1 + \dots + \alpha_{n(x)} e_{n(x)}$ ,  $\alpha_j \in \mathbb{Q}$ ,  $e_j \in \mathfrak{H}$ ,  $j = 1, \dots, n(x)$ ,  $n(x) \in \mathbb{N}$ ). Such a basis is known as a *Hamel base*. It is known that, without loss of generality, we may assume that  $\pi$  (i.e., the area of a unit disk in Euclidean 2-space) is an element of  $\mathfrak{H}$ . If we assume this, we can at once write down all  $\mathbb{Q}$ -linear functions  $f : \mathbb{R} \rightarrow \mathbb{R}$  such that  $f(\pi) = 0$ ; we put  $f(\pi) = 0$ , give  $f(e)$  arbitrary values for  $e \in \mathfrak{H}$ ,  $e \neq \pi$ , and define  $f(x)$  generally by  $f(x) = \alpha_1 f(e_1) + \dots + \alpha_n f(e_n)$  for  $x = \alpha_1 e_1 + \dots + \alpha_{n(x)} e_{n(x)}$ ,  $\alpha_j \in \mathbb{Q}$ ,  $e_j \in \mathfrak{H}$ ,  $j = 1, \dots, n(x)$ . Obviously, we can represent an arbitrary  $\mathbb{Q}$ -linear function  $f : \mathbb{R} \rightarrow \mathbb{R}$  such that  $f(\pi) = 0$  as  $f(x) = \sum p_e f_e(x)$ , where the sum is taken over all  $e \in \mathfrak{H}$ , except  $\pi$ ;  $p_e$  are arbitrary real numbers; and  $f_e(x) = \alpha_k$  provided  $x = \alpha_1 e_1 + \dots + \alpha_{n(x)} e_{n(x)}$  and  $e = e_k$ . The latter representation makes it clear that the following two statements are equivalent:

- (1) The Dehn invariant  $D_f$  remains constant during a flex for every  $\mathbb{Q}$ -linear function  $f : \mathbb{R} \rightarrow \mathbb{R}$  such that  $f(\pi) = 0$ ;
- (2) The Dehn invariant  $D_{f_e}$  remains constant during a flex for every dual element  $f_e$ , corresponding to  $e \in \mathfrak{H}$ ,  $e \neq \pi$ .

Note also that  $f_e(x)$  is a rational number for every  $x \in \mathbb{R}$  and every  $e \in \mathfrak{H}$ .

Let  $\mathcal{S}$  be a flexible suspension constructed in Section 3. Fix some  $e \in \mathfrak{H}$ ,  $e \neq \pi$ . Substituting the values of the edge lengths,  $|e_j|$ ,  $|e'_j|$ , and  $|e_{j,j+1}|$ , from Tables 4 and 5 to the expression of Dehn invariant

$$D_{f_e} = \sum_{j=1}^6 [f_e(\varphi_j(x))|e_j| + f_e(\varphi'_j(x))|e'_j| + f_e(\varphi_{j,j+1}(x))|e_{j,j+1}|]$$

yields

$$D_{f_e} = f_e(\alpha_1(x)) + f_e(\alpha_2(x))\sqrt{2} + f_e(\alpha_3(x))\sqrt{15} + f_e(\alpha_4(x))\sqrt{30} + f_e(\alpha_5(x))\sqrt{85} + f_e(\alpha_6(x))\sqrt{102} + f_e(\alpha_7(x))\sqrt{170},$$

where

$$(4.1) \quad \alpha_1(x) = \frac{541419683182996345}{29669606628505029} \varphi_{12}(x) + \frac{31635727886833754300}{1435086871311616559} \varphi_{23}(x)$$

$$\begin{aligned}
 & + \frac{27288800741}{19943076519} \varphi_{34}(x) + \frac{130585}{9603} \varphi_{45}(x) \\
 & + \frac{100}{11} \varphi_{56}(x) + \frac{310327}{472293} \varphi_{61}(x), \\
 (4.2) \quad \alpha_2(x) &= -\frac{1}{2}(\varphi_3(x) - \varphi'_3(x)) + \frac{1}{2}(\varphi_6(x) - \varphi'_6(x)),
 \end{aligned}$$

$$(4.3) \quad \alpha_3(x) = \frac{718}{541}(\varphi_1(x) + \varphi'_1(x)) + 2(\varphi_4(x) + \varphi'_4(x)),$$

$$(4.4) \quad \alpha_4(x) = -\frac{1}{2}(\varphi_2(x) - \varphi'_2(x)) - \frac{1}{2}(\varphi_5(x) - \varphi'_5(x)),$$

$$(4.5) \quad \alpha_5(x) = \frac{109}{873}(\varphi_1(x) - \varphi'_1(x)) - \frac{109}{873}(\varphi_4(x) - \varphi'_4(x)),$$

$$(4.6) \quad \alpha_6(x) = \frac{31054297}{45688606}(\varphi_3(x) + \varphi'_3(x)) + \frac{1}{2}(\varphi_6(x) + \varphi'_6(x)),$$

$$(4.7) \quad \alpha_7(x) = \frac{182493018091}{125640679106}(\varphi_2(x) + \varphi'_2(x)) + \frac{17}{22}(\varphi_5(x) + \varphi'_5(x)).$$

Since the numbers  $2, 15 = 3 \cdot 5, 30 = 2 \cdot 3 \cdot 5, 85 = 5 \cdot 17, 102 = 2 \cdot 3 \cdot 17,$  and  $170 = 2 \cdot 5 \cdot 17$  are square free it follows that the numbers  $1, \sqrt{2}, \sqrt{15}, \sqrt{30}, \sqrt{85}, \sqrt{102},$  and  $\sqrt{170}$  are linearly independent over rationals. Taking into consideration that  $f_e(\alpha_j(x))$  is rational for all  $x$  and  $j = 1, \dots, 7,$  we conclude that  $D_{f_e}$  is constant in  $x$  if and only if  $\alpha_j(x)$  is constant in  $x$  for every  $j = 1, \dots, 7.$

The rest of this article is devoted to the study of expressions  $\alpha_j(x).$

**Dihedral angles adjacent to  $p_2, p_4, p_5,$  and  $p_6.$**  By  $\mathcal{Q}_j, j = 1, \dots, 6,$  denote the intersection of suspension  $\mathcal{S}$  with a sphere centered at  $p_j$  of a radius so small that it contains no vertices of  $\mathcal{S}$  other than  $p_j.$  Note that, since  $\mathcal{S}$  admits two flat positions (which occur when the distance between the poles is 10 or  $\sqrt{51}),$  the spherical quadrangle  $\mathcal{Q}_j$  admits two ‘line’ positions, i.e., positions when all its vertices are contained in a great circle. From Figure 9 and Figure 10, we conclude that, for  $j = 2, 4, 5$  and 6, none of the ‘line’ positions of  $\mathcal{Q}_j$  coincides with a whole great circle. If we denote the side lengths of  $\mathcal{Q}_j$  by  $\omega_{j1}, \omega_{j2}, \omega_{j3},$  and  $\omega_{j4}$  in cyclic order then  $\mathcal{Q}_j$  can be drawn in one ‘line’ position as shown on Figure 12(a) and in another ‘line’ position as shown on



FIGURE 12. Two ‘line’ positions of the spherical quadrangle  $\mathcal{Q}_j.$

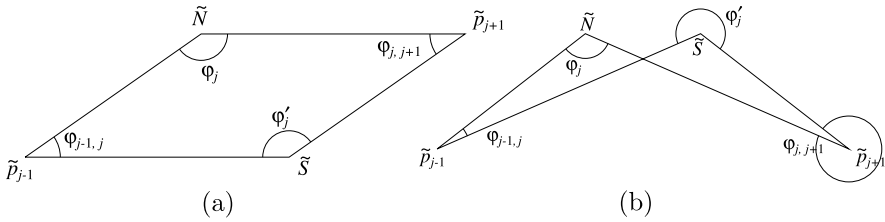


FIGURE 13. Two possibilities for the spherical quadrangle  $\mathcal{Q}_j$ : (a)  $\mathcal{Q}_j$  is a convex centrally symmetric quadrangle. (b)  $\mathcal{Q}_j$  is a non-convex quadrangle (with a point of self-intersection) symmetric with respect to a ‘line’.

Figure 12(b). It follows from Figure 12(a) that  $\omega_{j1} + \omega_{j2} = \omega_{j3} + \omega_{j4}$ . Similarly, it follows from Figure 12(b) that  $\omega_{j4} + \omega_{j1} = \omega_{j2} + \omega_{j3}$ . Solving these two linear equations, we get  $\omega_{j2} = \omega_{j4}$  and  $\omega_{j1} = \omega_{j3}$ .

In other words, the latter means that, for  $j = 2, 4, 5$ , and  $6$ , the opposite sides of  $\mathcal{Q}_j$  are pairwise equal to each other. Under these conditions,  $\mathcal{Q}_j$  may be either a convex centrally symmetric quadrangle, see Figure 13(a), or a non-convex quadrangle (with a point of self-intersection) symmetric with respect to a ‘line’, i.e., to a great circle, see Figure 13(b). On Figure 13, we denote the intersection of edge  $\langle p_j, X \rangle$  with the small sphere centered at  $p_j$  by  $\tilde{X}$ .

Recall from Section 2 that, by definition,  $\varepsilon_{j,j+1}$  equals the sign of  $(e_j \times e_{j+1}) \cdot R$ . Equivalently,  $\varepsilon_{j,j+1}$  equals the sign of  $\theta_{j,j+1}$ . This means that if  $\varepsilon_{j-1,j}\varepsilon_{j,j+1} < 0$  then tetrahedra  $\langle N, p_{j-1}, p_j, S \rangle$  and  $\langle N, p_j, p_{j+1}, S \rangle$  lie on the same side of the plane which passes through the points  $N, p_j$ , and  $S$ . In this case  $\mathcal{Q}_j$  is a non-convex spherical quadrangle whose opposite sides are pairwise equal to each other as show on Figure 13(b) and the sum of opposite angles of  $\mathcal{Q}_j$  equals  $2\pi$ . In terms of multi-valued functions, we may write

$$(4.8) \quad \varphi'_j(x) = -\varphi_j(x) \quad \text{and} \quad \varphi_{j-1,j}(x) = -\varphi_{j,j+1}(x) \quad \text{for all } x.$$

From Table 3, we read  $\varepsilon_{12} = \varepsilon_{45} = \varepsilon_{61} = -1$  and  $\varepsilon_{23} = \varepsilon_{34} = \varepsilon_{56} = +1$ . Thus,  $\varepsilon_{12}\varepsilon_{23}\varepsilon_{34}\varepsilon_{45} = \varepsilon_{45}\varepsilon_{56}\varepsilon_{56}\varepsilon_{61} = -1 < 0$  and  $\mathcal{Q}_j$  is a non-convex quadrilateral for  $j = 2, 4, 5$  and  $6$ , as described above and (4.8) holds for the same  $j$ 's.

Let us summaries the relations obtained as follows

$$(4.9) \quad \begin{array}{ll} \varphi_{23}(x) = -\varphi_{12}(x), & \varphi'_2(x) = -\varphi_2(x), \\ \varphi_{45}(x) = -\varphi_{34}(x), & \varphi'_4(x) = -\varphi_4(x), \\ \varphi_{56}(x) = -\varphi_{45}(x), & \varphi'_5(x) = -\varphi_5(x), \\ \varphi_{61}(x) = -\varphi_{56}(x), & \varphi'_6(x) = -\varphi_6(x). \end{array} \quad \text{and}$$

**Dihedral angles adjacent to  $p_1$  and  $p_3$ .** Unfortunately, we cannot apply the arguments from the previous subsection to  $\mathcal{Q}_1$  and  $\mathcal{Q}_3$ , because in the

flat position shown on Figure 9 each of these spherical quadrangles coincides with a great circle. This is the reason why we use other arguments in this subsection.

Using the Euclidean Cosine Law and the exact values of side lengths of triangles  $\langle N, p_1, p_2 \rangle$ ,  $\langle S, p_1, p_2 \rangle$ ,  $\langle S, p_1, p_6 \rangle$ , and  $\langle N, p_1, p_6 \rangle$  given in Tables 4 and 5, we find

$$\begin{aligned}\cos \angle N p_1 p_2 &= \frac{7(-3200524333319476 + 9569278607860305\sqrt{51})}{319877868986(626814\sqrt{15} + 58969\sqrt{85})}; \\ \cos \angle S p_1 p_2 &= -\frac{7(3200524333319476 + 9569278607860305\sqrt{51})}{319877868986(626814\sqrt{15} - 58969\sqrt{85})}; \\ \cos \angle S p_1 p_6 &= \frac{1565240 - 472293\sqrt{51}}{1253628\sqrt{15} - 117938\sqrt{85}}; \\ \cos \angle N p_1 p_6 &= \frac{1565240 + 472293\sqrt{51}}{1253628\sqrt{15} + 117938\sqrt{85}}.\end{aligned}$$

Now direct calculations show that

$$\arccos \angle N p_1 p_2 + \arccos \angle S p_1 p_6 + \arccos \angle S p_1 p_2 + \arccos \angle N p_1 p_6 = 0.$$

Hence,

$$(4.10) \quad \angle N p_1 p_2 + \angle S p_1 p_6 = \angle S p_1 p_2 + \angle N p_1 p_6 = \pi.$$

Consider spherical quadrangle  $\mathcal{Q}_1 = \langle \tilde{N}, \tilde{p}_2, \tilde{S}, \tilde{p}_6 \rangle$  as being composed of two spherical triangles  $\langle \tilde{N}, \tilde{S}, \tilde{p}_6 \rangle$  and  $\langle \tilde{N}, \tilde{S}, \tilde{p}_2 \rangle$ . Using the Spherical Cosine Law [5, Theorem 18.6.8] and (4.10), we get

$$\cos \angle \tilde{p}_2 = \frac{\cos \tilde{N}\tilde{S} - \cos \tilde{S}\tilde{p}_2 \cos \tilde{N}\tilde{p}_2}{\sin \tilde{S}\tilde{p}_2 \sin \tilde{N}\tilde{p}_2} = \frac{\cos \tilde{N}\tilde{S} - \cos \tilde{S}\tilde{p}_6 \cos \tilde{N}\tilde{p}_6}{\sin \tilde{S}\tilde{p}_6 \sin \tilde{N}\tilde{p}_6} = \cos \angle \tilde{p}_6,$$

where  $\tilde{N}\tilde{S}$  stands for the spherical distance between points  $\tilde{N}$  and  $\tilde{S}$  and  $\angle \tilde{p}_2$  stands for the angle of  $\mathcal{Q}_1$  at vertex  $\tilde{p}_2$ .

Note that some branch of multi-valued function  $\varphi_{12}(x)$  equals  $\angle \tilde{p}_2$  or  $2\pi - \angle \tilde{p}_2$  for  $\mathcal{Q}_1$  constructed for the same value of  $x$ . Similarly, some branch of  $\varphi_{61}(x)$  equals  $\angle \tilde{p}_6$  or  $2\pi - \angle \tilde{p}_6$ . Taking into account that  $\varepsilon_{61} = \varepsilon_{12} = -1$  and, thus, the suspension  $\mathcal{S}$  is either convex or concave at edges  $e_{61}$  and  $e_{12}$  simultaneously, we conclude that

$$(4.11) \quad \varphi_{61}(x) = \varphi_{12}(x) \quad \text{for all } x.$$

Applying the same arguments to  $\mathcal{Q}_1$  treated as being composed of the triangles  $\langle \tilde{N}, \tilde{p}_2, \tilde{p}_6 \rangle$  and  $\langle \tilde{S}, \tilde{p}_2, \tilde{p}_6 \rangle$  and taking into account that  $\mathcal{Q}_1$  is convex only if it is flat, we get

$$(4.12) \quad \varphi_1'(x) = -\varphi_1(x) \quad \text{for all } x.$$

Using similar arguments for  $\mathcal{Q}_3$ , we obtain for all  $x$

$$(4.13) \quad \varphi_{23}(x) = \varphi_{34}(x) \quad \text{and} \quad \varphi'_3(x) = -\varphi_3(x).$$

$\alpha_j(x)$  is constant in  $x$  for  $j = 1, 3, 6$ , and 7 and is not constant for  $j = 4$ . Substituting (4.9) and (4.11)–(4.13) to (4.1)–(4.7) we obtain

$$(4.14) \quad \alpha_1(x) = \left( \frac{541419683182996345}{29669606628505029} - \frac{31635727886833754300}{1435086871311616559} - \frac{27288800741}{19943076519} + \frac{130585}{9603} - \frac{100}{11} + \frac{310327}{472293} \right) \varphi_{12}(x) + \text{const},$$

$$\alpha_2(x) = -\varphi_3(x) + \varphi_6(x),$$

$$\alpha_3(x) = \text{const},$$

$$\alpha_4(x) = -\varphi_2(x) - \varphi_5(x),$$

$$\alpha_5(x) = \frac{218}{873}(\varphi_1(x) - \varphi_4(x)),$$

$$\alpha_6(x) = \text{const},$$

$$\alpha_7(x) = \text{const}.$$

Note that, due to (3.8), the right-hand side of (4.14) is, in fact, constant in  $x$ . Hence,  $\alpha_j(x)$  is constant in  $x$  for  $j = 1, 3, 6$ , and 7. On the other hand, we know enough about dihedral angles of  $\mathcal{S}$  to prove that  $\alpha_4(x)$  or, equivalently,  $\varphi_2(x) + \varphi_5(x)$  is not constant.

Recall that Figure 10 represents suspension  $\mathcal{S}$  in a flat position which corresponds to  $x = 51$ . In the moment, restrict our study by spatial forms of  $\mathcal{S}$  which are close enough to that flat position; in particular, assume that

- (i) univalent branches of multivalued functions  $\varphi_j(x)$ ,  $\varphi'_j(x)$ , and  $\varphi_{j,j+1}(x)$  are chosen which take values shown on Table 6 for  $x = 51$  and
- (ii) the absolute value of the branch of  $\varphi_{12}(x)$  is so small that throughout our discussion there is no necessity to switch to other branches.

Taking into account relations (4.9), (4.11), and (4.13) and using Figure 10, we draw spherical quadrangles  $\mathcal{Q}_2$  and  $\mathcal{Q}_5$  on Figures 14 and 15, respectively.

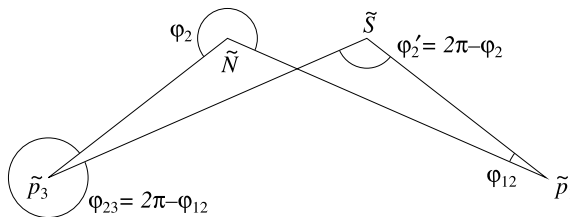
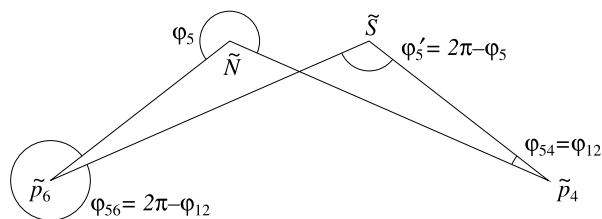


FIGURE 14. Spherical quadrangle  $\mathcal{Q}_2$ .

FIGURE 15. Spherical quadrangle  $\mathcal{Q}_5$ .

An obvious consequence of Figures 14 and 15 is that both  $\varphi_2(x)$  and  $\varphi_5(x)$  increase as  $\varphi_{12}(x)$  increases. Hence, the sum  $\varphi_2(x) + \varphi_5(x)$  is not constant. This implies that  $\alpha_4(x)$  and Dehn invariant  $D_{f_e}$  are not constant and, thus, we have proven the following theorem.

**THEOREM.** *The suspension  $\mathcal{S}$  with a hexagonal equator constructed in Section 3 provides us with a counterexample to the Strong Bellows Conjecture.*

**Discussion.** Note that the Strong Bellows Conjecture holds for every flexible suspension with a quadrilateral equator (i.e., for every Bricard flexible octahedron) [2].

We conjecture that the Strong Bellows Conjecture is wrong even for embedded polyhedra and that a counterexample can be constructed by elimination of self-intersections in a counterexample for the Strong Bellows Conjecture in a way similar to that was used by R. Connelly in [8].

Just note that if the Strong Bellows Conjecture holds for a polyhedron  $\mathcal{P}$  (for example, because  $\mathcal{P}$  is not flexible) and is wrong for a polyhedron  $\mathcal{Q}$  (for example, consider suspension  $\mathcal{S}$  constructed in Section 3) then it is wrong for a polyhedron  $\mathcal{R}$  obtained by gluing  $\mathcal{P}$  and  $\mathcal{Q}$  along a pair of isometric faces. In particular, if  $\mathcal{R}$  is embedded (i.e., has no self-intersections) we obtain a counterexample to the Strong Bellows Conjecture for embedded polyhedra.

Unfortunately, we cannot realize this idea right now because the suspension  $\mathcal{S}$  is more complicated object than the Bricard's flexible octahedron used in [8]. Roughly speaking, Bricard's octahedron in a flat position is a twice-covered polygon, while some parts of  $\mathcal{S}$  in a flat position shown on Figure 9 are four-covered.

Finally, we underline that the flexible suspension  $\mathcal{S}$  has surprisingly many hidden symmetries in edges and dihedral angles.

**Acknowledgment.** The first author expresses his gratitude for the hospitality of the Department of Mathematics of Cornell University during his visit in 2007 when part of this paper was written.

## REFERENCES

- [1] R. Alexander, *Lipschitzian mappings and total mean curvature of polyhedral surfaces, I*, Trans. Amer. Math. Soc. **288** (1985), 661–678. MR 0776397
- [2] V. Alexandrov, *The Dehn invariants of the Bricard octahedra*, J. Geom. **99** (2010), 1–13. MR 2823098
- [3] F. J. Almgren and I. Rivin, *The mean curvature integral is invariant under bending, The Epstein birthday schrift* (I. Rivin et al., eds.), University of Warwick, Warwick, 1998, pp. 1–21. MR 1668323
- [4] C. Berge, *Graphs and hypergraphs*, North-Holland, Amsterdam, 1973. MR 0357172
- [5] M. Berger, *Geometry. II*, Springer, Berlin, 1987. MR 0882916
- [6] V. G. Boltyanskii, *Hilbert's third problem*, Winston & Sons, Washington, DC, 1978. MR 0500434
- [7] R. Connelly, *An attack on rigidity I, II*, preprint, 1974, pp. 1–36; 1–28. (Available at: <http://www.math.cornell.edu/~connelly>. Russian translation in the book: A. N. Kolmogorov, S. P. Novikov (eds.), *Issledovaniya po metricheskoj teorii poverkhnostej*, Mir, Moscow, 1980, pp. 164–209. MR 0608632) An abridged version: R. Connelly, *An attack on rigidity*, Bull. Amer. Math. Soc. **81** (1975), 566–569. MR 0388288
- [8] R. Connelly, *A counterexample to the rigidity conjecture for polyhedra*, Inst. Hautes Études Sci. Publ. Math. **47** (1977), 333–338. MR 0488071
- [9] R. Connelly, I. Sabitov and A. Walz, *The bellows conjecture*, Beiträge Algebra Geom. **38** (1997), 1–10. MR 1447981
- [10] H. Hadwiger, *Vorlesungen über Inhalt, Oberfläche und Isoperimetrie*, Springer, Berlin, 1957. MR 0102775
- [11] F. Harary, *Graph theory*, Addison-Wesley, Reading, MA, 1969. MR 0256911
- [12] S. Lang, *Elliptic functions*, Springer, New York, 1987. MR 0890960
- [13] S. N. Mikhalev, *Some necessary metric conditions for flexibility of suspensions*, Mosc. Univ. Math. Bull. **56** (2001), 14–20. MR 1863550
- [14] I. Kh. Sabitov, *Local theory on bendings of surfaces*, Geometry III. Theory of surfaces. Encycl. Math. Sci., vol. 48, Springer, Berlin, 1992, pp. 179–250. MR 1306736
- [15] I. Kh. Sabitov, *The volume of a polyhedron as a function of its metric* (in Russian), Fundam. Prikl. Mat. **2** (1996), 1235–1246. MR 1785783
- [16] I. Kh. Sabitov, *The volume as a metric invariant of polyhedra*, Discrete Comput. Geom. **20** (1998), 405–425. MR 1651896
- [17] R. Walker, *Algebraic curves*, Princeton Univ. Press, Princeton, NJ, 1950. MR 0033083

VICTOR ALEXANDROV, SOBOLEV INSTITUTE OF MATHEMATICS, NOVOSIBIRSK, RUSSIA AND DEPARTMENT OF PHYSICS, NOVOSIBIRSK STATE UNIVERSITY, NOVOSIBIRSK, 630090, RUSSIA  
E-mail address: alex@math.nsc.ru

ROBERT CONNELLY, DEPARTMENT OF MATHEMATICS, MALOTT HALL, CORNELL UNIVERSITY, ITHACA, NY 14853, USA

E-mail address: rc46@cornell.edu